Generalized Code-Multiplexing for UWB Communications

Qi Zhou, Xiaoli Ma, and Vincenzo Lottici

Abstract—Code-multiplexed transmitted reference (CM-TR) and code-shifted reference (CSR) have recently drawn attention in the field of ultra-wideband communications mainly because they enable noncoherent detection without requiring either a delay component, as in transmitted reference, or an analog carrier, as in frequency-shifted reference, to separate the reference and data-modulated signals at the receiver. In this paper, we propose a generalized code-multiplexing (GCM) system based on the formulation of a constrained mixed-integer optimization problem. The GCM extends the concept of CM-TR and CSR while retaining their simple receiver structure, even offering better bit-error-rate performance and a higher data rate in the sense that more data symbols can be embedded in each transmitted block. The GCM framework is further extended to the cases when peak power constraint is considered and when inter-frame interference exists, as typically occurs in high data-rate transmissions. Numerical simulations performed over demanding wireless environments corroborate the effectiveness of the proposed approach.

Index Terms—UWB communications, noncoherent detectors, transmitted reference, code-multiplexing

I. INTRODUCTION

In ultra-wideband (UWB) impulse radio (IR) signaling, information is conveyed by transmitting sequences of ultra-short pulses at very low power spectrum density [1]–[3]. After traveling through multipath channels [4]–[6], each transmitted pulse appears at the receiver as hundreds of echoes. To collect the energy through these multiple paths, Rake receivers are proposed in [7], [8]; however, they exhibit high complexity due to a large number of fingers together with intensive computational cost and extremely high sampling rate required in estimating the amplitude and the delay of the channel paths [9]. As a sub-optimal yet simple solution, transmitted reference (TR) systems avoid channel estimation by transmitting each information symbol through two pulses, namely the (unmodulated) reference and the data pulses [8], [10]–[13], [29], [30]. Thus, the received reference pulses allow the recovery of the noisy channel template, which is then employed for data detection based on a correlation scheme. The TR concept enables simple receiver structures, but the delay component required by the correlation unit, amounting to tens or even hundreds of nanoseconds, presents a non negligible drawback in terms of hardware implementation. In both cases, the delay componenet is built via either analog circuitry or digital sampling [14]–[16]. A viable alternative to the TR scheme for efficient energy capture is based on differential detection (DD), as pursued originally in [17], [28] and in a few improved multi-symbol differential detection (MSDD) [18], [19]. These detectors are attractive in that they can efficiently gather energy from all the multiple paths; however, they still suffer from the need for accurate delay lines on the order of multiples of symbol intervals.

Relations with prior work. To overcome the implementation issue posed by the delay components, the frequency-shifted reference (FSR) system has been proposed to separate the reference and data-modulated signals in the frequency domain at the price of requiring an analog carrier [20]. The FSR is further simplified by the code-multiplexed TR (CM-TR) [21] and code-shifted reference (CSR) [22] schemes based on orthogonal code sequence design. Noteworthy, both systems are promising schemes as they require neither delay elements nor analog carriers, while even exhibiting better bit error rate (BER) performance compared to the FSR solution.

Purpose and contributions. The aim of this paper is to generalize the CM-TR and CSR concepts through a novel design we refer to as "generalized code-multiplexing," or GCM for short in the following. The rationale of the proposed transmitter and receiver structure relies on the formulation of a constrained optimization problem (OP), which maximizes the BER performance metric under a given set of constraints mainly adopted to keep complexity at affordable levels. Several features differentiate the proposed approach from previous work and define our contributions.

1) The GCM inherits the basic structure of the CM-TR and CSR systems based on a simple energy detector without any delay line components. As a further step, however, after solving offline a joint OP on the transmitted and decoding codes for a given frame size N_f and number of information symbols M conveyed within each block, improved BER link performance and higher spectral efficiency are enabled.

2) When the frame size $N_f > 2^M$, the non-deterministic polynomial hard (NP-hard) nature of the original constrained OP can circumvented by deriving the closed-form optimal solution from an equivalent system with $N_f = 2^M$.

3) To take account of the emission power restriction imposed by the Federal Communications Commission (FCC) for UWB communications, we develop the GCM systems with peak power constraint, which can maintain

Q. Zhou and X. Ma are with the School of Electrical and Computer Engineering, Georgia Institute of Technology, Atlanta, GA, 30332 (e-mail: {qzhou32, xiaoli}@ece.gatech.edu).

V. Lottici is with the Department of Information Engineering, University of Pisa, Pisa, I-56122 Italy (e-mail: vincenzo.lottici@iet.unipi.it).

the same error performance as the existing designs while enjoying lower peak power levels.

4) The GCM framework is then extended to the more general case when inter-frame interference (IFI) arises, as typically occurs in high data rate transmissions. Through the formulation of an OP based on a properly modified signal model, the IFI effects can be mitigated, and thus obtaining a considerable performance improvement compared to some existing codes.

Organization. The rest of the paper is organized as follows. Sec. II describes the system model, Sec. III introduces the GCM optimization problem, and Sec. IV extends the proposed code sequence design to transmissions with IFI. Sec. V first gives an example of the optimization results and then compares the BER performance of the GCM for various setups, taking the conventional CSR as a benchmark. Finally, Sec. VI concludes the paper.

Notations. Matrices are in upper case bold while column vectors are in lower case bold, $(\cdot)^T$ denotes the transpose, $[\mathbf{A}]_{m,n}$ denotes the (m,n)th entry of the matrix $\mathbf{A}$, $\mathbf{a}^{(i)}$ denotes the ith row of matrix $\mathbf{A}$, $\odot$ denotes the Hadamard element-by-element vector multiplication, $\otimes$ denotes the Kronecker product, $\mathrm{diag}(\cdot)$ converts a sequence of size N into an $N \times N$ diagonal matrix, $\star$ denotes linear convolution, $\lceil \cdot \rceil$ denotes the ceiling function, $\triangleq$ stands for definition, $\mathbf{A}_{N \times L}$ denotes an $N \times L$ matrix, $\mathbf{I}_N$ denotes the $N \times N$ identity matrix, $\mathbf{J}_N$ denotes an $N \times N$ matrix with 1 below the main diagonal and 0 elsewhere, $\mathbf{0}_{N \times L}$ is the $N \times L$ matrix with all entries zero, $\mathbf{1}_{N \times L}$ is the $N \times L$ matrix with all entries one, and $\mathrm{sgn}(x)$ is the sign function, which takes values -1 and 1 depending on the polarity of the argument. $\mathrm{E}\{\cdot\}$ denotes statistical expectation, and $\mathrm{Var}\{\cdot\}$ denotes statistical variance.

II. SYSTEM MODEL

Consider the GCM system depicted in Fig. 1. A sequence of M information symbols $\mathbf{a} \triangleq [a_1, \cdots, a_M]^T, a_i \in \{\pm 1\}$ are encoded at the transmitter into a block of N_f frame symbols $\mathbf{b} \triangleq [b_0, \cdots, b_{N_f-1}]^T$ according to the rule $\mathbf{b} = \boldsymbol{\chi}(\mathbf{a})$, $\boldsymbol{\chi} \triangleq [\chi_0, \chi_1, \cdots, \chi_{N_f-1}]^T$. Thus, the transmitted signal corresponding to the data block $\mathbf{a}$ can be written as

$$x(t) = \sum_{j=0}^{N_f-1} b_j p(t - jT_f), \qquad (1)$$

where $p(t)$ is the Gaussian monocycle pulse with duration T_p, N_f is the number of frames in the block, and T_f is the frame interval. Note that, for the time being, inter-frame interference (IFI) is avoided by choosing $T_f > T_m + T_p$, where T_m is defined as the maximum excess delay of the channel; however this assumption will be dropped in Sec. IV. For the sake of notational simplicity, we do not explicitly consider the typical frame structure for time hopping (TH) in that it can be removed at the receiver prior to further signal processing without incurring IFI under the condition of sufficiently long T_f.

The UWB propagation channel is assumed to be highly frequency-selective with the channel impulse response (CIR)

modeled as

$$h(t) = \sum_{n=0}^{N_p-1} \alpha_n \delta(t - \tau_n), \qquad (2)$$

where N_p is the total number of paths with amplitude α_n and delay τ_n. The channel coherence time, wherein the CIR stays approximately constant, is assumed to be longer than the block transmission interval $T_b = T_f N_f$.

After processing the received signal with a low-pass filter[1] having impulse response $h_{\mathrm{LP}}(t)$, which eliminates the out-of-band (OOB) interference and noise, in correspondence of (1), we obtain

$$y(t) = \sum_{j=0}^{N_f-1} b_j g(t - jT_f) + w(t), \qquad (3)$$

where $w(t)$ is a band-limited additive white Gaussian noise (AWGN) component with two-sided power spectrum density $N_0/2$, and the channel template $g(t) \triangleq p(t) \star h(t) \star h_{\mathrm{LP}}(t)$ has frame energy $E_f \triangleq \int_0^{T_m+T_p} g^2(t)dt$.

Under the assumption that timing has been acquired, energy integration is performed on the received signal

$$r_j = \int_{jT_f}^{(j+1)T_f} y^2(t)dt, \quad j \in \mathcal{J}, \qquad (4)$$

with $\mathcal{J} \triangleq \{0, \cdots, N_f - 1\}$. Then, the decision variable for the kth information symbol is obtained as

$$z_k = \mathbf{c}_k^T \mathbf{r}, \quad k \in \mathcal{K}, \qquad (5)$$

where $\mathbf{c}_k \triangleq [c_{k,0}, c_{k,1}, \cdots, c_{k,N_f-1}]^T$ is the decoding vector, $\mathbf{r} \triangleq [r_0, r_1, \cdots, r_{N_f-1}]^T$ includes the outputs in (4), and $\mathcal{K} \triangleq \{1, \cdots, M\}$. As a final step, the estimate of the information symbol is given by

$$\hat{a}_k = \mathrm{sgn}(z_k), \quad k \in \mathcal{K}. \qquad (6)$$

The system model in Eqs. (1), (3)-(6) subsumes some existing code-multiplexed (CM) designs.

1) *Code-Multiplexed Transmitted Reference (CM-TR)* The CM-TR system transmits the reference and the data-modulated signals together with $M = 1$ [21]. The CM-TR encoder is specified by

$$b_j = \chi_j(a_1) = d_j + a_1 u_j, \quad j \in \mathcal{J}, \qquad (7)$$

where the codewords $\mathbf{d} \triangleq [d_0, d_1, \cdots, d_{N_f-1}]^T$ and $\mathbf{u} \triangleq [u_0, u_1, \cdots, u_{N_f-1}]^T$ used for the reference and the data-modulated signals, respectively, have the properties: *i)* $d_j, u_j \in \{\pm 1\}$, $j \in \mathcal{J}$; and *ii)* they are orthogonal, i.e., $\mathbf{d}^T \mathbf{u} = 0$. At the receiver, the integrator output $\mathbf{r}$, after being correlated by the decoding vector $\mathbf{c}_1 = \mathbf{d} \odot \mathbf{u}$, yields the decision variable for the information symbol transmitted at each block. Note that, in fact, the CM-TR system can be considered as a generalized binary pulse position modulation (B-PPM) [31].

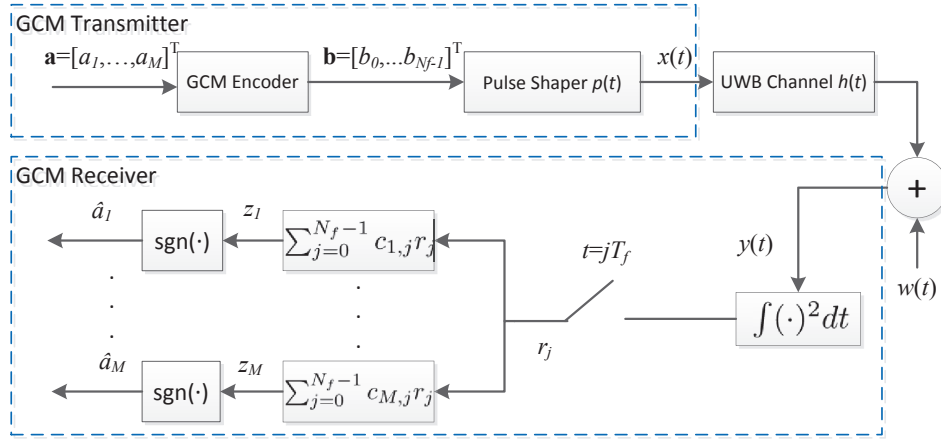[1] A quite similar system model holds in the case of employing a bandpass filter.

Fig. 1. System diagram of a block transmission for GCM systems

2) *Code-Shifted Reference (CSR)* In the CSR system, $M \geq 1$ information symbols $\mathbf{a}$ are transmitted into N_f frames according to the encoding rule [22]

$$b_j = \chi_j(\mathbf{a}) = \sqrt{M} v_{0,j} + \sum_{k=1}^{M} a_k v_{k,j}, \quad j \in \mathcal{J}, \quad (8)$$

where among the transmitted codewords $\mathbf{v}_k \triangleq [v_{k,0}, v_{k,1}, \cdots, v_{k,N_f-1}]^T, k \in \{0\} \cup \mathcal{K}$, the codeword with $k = 0$ ($\mathbf{v}_0$) is for the reference signal, whereas those for $k \in \mathcal{K}$ are used for the M information symbols. For data detection, the transmitted codewords $\mathbf{v}_k$ and decoding vectors $\mathbf{c}_k$ are chosen such that the following conditions are satisfied:

C1) $c_{k,j}, v_{i,j} \in \{\pm 1\}, k \in \mathcal{K}, j \in \mathcal{J}, i \in \{0\} \cup \mathcal{K}$;
C2) $\sum_{j=0}^{N_f-1} c_{k,j} = 0, k \in \mathcal{K}$;
C3) $\mathbf{c}_k^T(\mathbf{v}_0 \odot \mathbf{v}_i) = \begin{cases} N_f, & i = k, k \in \mathcal{K} \\ 0, & i \neq k, i \in \{0\} \cup \mathcal{K}, k \in \mathcal{K} \end{cases}$;
C4) $\mathbf{c}_k^T(\mathbf{v}_i \odot \mathbf{v}_j) = 0, \forall i, j, k \in \mathcal{K}$.

The following comments are worth emphasizing.

a) To comply with C1)-C4), Walsh codes are employed for $\mathbf{v}_k$ and $\mathbf{c}_k$ in [22, Table 1].

b) At most, $M = N_f/2$ information symbols can be encoded into N_f frames. This is because, for the Walsh codes with length 2^N, there exist, at most, $2^{N-1} + 1$ transmitted codewords and 2^{N-1} decoding vectors that satisfy conditions C1)-C4).

III. GCM OPTIMAL DESIGN

In this section, we formulate a constrained OP to design the GCM encoder $\mathbf{b} = \chi(\mathbf{a})$ and decoding matrix $\mathbf{C} \triangleq [\mathbf{c}_1, \cdots, \mathbf{c}_M]$ so that the link performance in terms of the BER metric is optimized under a given set of assumptions.

A. Formulation of GCM Systems

Let us first define the GCM system we are dealing with, which subsumes CM-TR and CSR as special cases.

Definition 1: A transmitter with encoder $\mathbf{b} = \chi(\mathbf{a})$ and a receiver with decoding matrix $\mathbf{C}$ form a GCM system if the following assumptions are satisfied:

A1) $c_{k,j} \in \{\pm 1\}, k \in \mathcal{K}, j \in \mathcal{J}$;
A2) $\sum_{j=0}^{N_f-1} c_{k,j} = 0, k \in \mathcal{K}$;
A3) The error probabilities on $a_k, k \in \mathcal{K}$ are equal.

Then, we derive an equivalent definition of the GCM system that will be particularly useful to formulate the GCM OP. To be specific, we take the conditions of both the absence of IFI and sufficiently large product BT_f, B being the bandwidth of the receiver low-pass filter $h_{\mathrm{LP}}(t)$.

Proposition 1: A GCM system with encoder $\mathbf{b} = \chi(\mathbf{a})$ and decoding matrix $\mathbf{C}$ holds if assumption A3) is replaced by A3a)-A3b) as:

A1) $c_{k,j} \in \{\pm 1\}, k \in \mathcal{K}, j \in \mathcal{J}$;
A2) $\sum_{j=0}^{N_f-1} c_{k,j} = 0, k \in \mathcal{K}$;
A3a) $\mathbf{c}_k^T(\mathbf{b}_i \odot \mathbf{b}_i) = \Psi \, a_{i,k}, i \in \mathcal{I}, k \in \mathcal{K}$;
A3b) $\|\mathbf{b}_i\|_2^2 = E_\mathbf{b}, i \in \mathcal{I}$,

where $\mathbf{a}_i \triangleq [a_{i,1}, \cdots, a_{i,M}]^T$ and $\mathbf{b}_i \triangleq [b_{i,0}, \cdots, b_{i,N_f-1}]^T$, with $i \in \mathcal{I} \triangleq \{1, \cdots, 2^M\}$, denote the realizations of the information symbol $\mathbf{a}$ and the transmitted symbol $\mathbf{b}$, respectively, with $\mathbf{b}_i = \chi(\mathbf{a}_i)$; $E_\mathbf{b}$ is the energy of the transmitted symbol $\mathbf{b}_i$, assumed to be constant $\forall i \in \mathcal{I}$; and Ψ is a parameter that strictly depends on both the encoding rule $\mathbf{b} = \chi(\mathbf{a})$ and the decoding matrix $\mathbf{C}$.

Proof: See Appendix A. ∎

Now, a key result about the GCM system is ready to be derived, as stated in the sequel.

Proposition 2: Assuming a GCM system with encoder $\chi(\mathbf{a})$ and decoding matrix $\mathbf{C}$ satisfying Proposition 1, the BER performance is asymptotically approximated in terms of the twice time-bandwidth product $L \triangleq \lceil 2BT_f \rceil$ when L is large as

$$\mathrm{BER}_{\mathrm{GCM}}(\Omega) = Q\left[\Omega\left(\frac{2M}{\gamma} + \frac{N_f L}{2\gamma^2}\right)^{-1/2}\right], \quad (9)$$

where $\Omega \triangleq M\Psi/E_\mathbf{b}$, $\gamma \triangleq E_{bit}/N_0$ is the received-bit-energy-to-noise-spectral-density ratio, and $Q(x) \triangleq \frac{1}{\sqrt{2\pi}} \int_x^\infty \exp(-t^2/2) dt$.

Proof: See Appendix B. ∎

Given Propositions 1-2, we are now ready to establish the relationship between our GCM systems and existing systems.

Corollary 1: The CM-TR system is a GCM system with $M = 1$ and $\Omega = 1$.

Proof: First, it can be shown that assumptions A1)-A2) hold for the CM-TR system as well. The entries of the decoding vector $\mathbf{c}_1 = \mathbf{d} \odot \mathbf{u}$ take values in $\{\pm 1\}$, while

$$\sum_{j=0}^{N_f-1} c_{1,j} = \mathbf{d}^T \mathbf{u} = 0. \qquad (10)$$

Then, the signal component in the decision variable $z_1 = \mathbf{c}_1^T \mathbf{r}$ can be rearranged as

$$\mathbf{c}_1^T(\mathbf{b} \odot \mathbf{b}) = (\mathbf{d} \odot \mathbf{u})^T \left[(\mathbf{d} + a_1 \mathbf{u}) \odot (\mathbf{d} + a_1 \mathbf{u}) \right]$$
$$= 2(\mathbf{d} \odot \mathbf{u})^T \left[\mathbf{1}_{N_f \times 1} + a_1 (\mathbf{d} \odot \mathbf{u}) \right] = 2N_f a_1, \qquad (11)$$

and the energy of the transmitted symbols $\mathbf{b}_1$ (corresponding to a_1) becomes

$$E_{\mathbf{b}} = \|\mathbf{b}_1\|_2^2 = (\mathbf{d} + a_1 \mathbf{u})^T (\mathbf{d} + a_1 \mathbf{u}) = 2N_f, \qquad (12)$$

which indicates that assumptions A3a)-A3b) hold. Therefore, by exploiting the results derived in the proof of Propositions 1-2, we conclude that the CM-TR system is a special case of GCM systems with $\Omega = 1$. ∎

Corollary 2: The CSR system is equivalent to a GCM system with $\Omega = \sqrt{M}$.

Proof: In order to prove the equivalence between the CSR under C1)-C4) and the GCM under A1)-A3b) for a particular objective value Ω, let us start by replacing the expression obtained from (8) for a generic realization of the transmitted symbols $\mathbf{b} = \sqrt{M}\mathbf{v}_0 + \sum_{i=1}^{M} a_i \mathbf{v}_i$ into the signal component at the integrator output given by A3a). Thus, applying conditions C3)-C4) yields

$$\mathbf{c}_k^T(\mathbf{b} \odot \mathbf{b}) = M\mathbf{c}_k^T(\mathbf{v}_0 \odot \mathbf{v}_0) + 2\sqrt{M} \sum_{i=1}^{M} a_i \mathbf{c}_k^T(\mathbf{v}_0 \odot \mathbf{v}_i)$$
$$+ \sum_{i=1}^{M} \sum_{j=1}^{M} a_i a_j \mathbf{c}_k^T(\mathbf{v}_i \odot \mathbf{v}_j) = 2\sqrt{M} N_f a_k, \quad k \in \mathcal{K}, \qquad (13)$$

which indicates that assumption A3a) holds for the CSR as well, with $\Psi = 2\sqrt{M} N_f$. Furthermore, due to the property $\mathbf{v}_i^T \mathbf{v}_j = 0$, $i \neq j$, exhibited by the Walsh codes, we obtain

$$E_{\mathbf{b}} = \|\mathbf{b}\|_2^2 = \left(\sqrt{M}\mathbf{v}_0 + \sum_{j=1}^{M} a_j \mathbf{v}_j \right)^T \left(\sqrt{M}\mathbf{v}_0 + \sum_{i=1}^{M} a_i \mathbf{v}_i \right)$$
$$= 2MN_f, \qquad (14)$$

which proves that the CSR also satisfies A3b). As a result, in view of the proof of Propositions 1-2, the CSR system is a special case of GCM systems with $\Omega = \sqrt{M}$. ∎

B. Optimization Problem for GCM Systems

According to Proposition 2, it can be recognized that given N_f, M, and L the BER performance metric is optimized whenever the encoder $\mathbf{b} = \chi(\mathbf{a})$ and the decoding matrix $\mathbf{C}$ are designed so that Ω in (9) is maximized under assumptions

A1)-A3b). Hence, Ω is just the objective function of the OP we are addressing. As such, in light of A3a), it will be denoted in the sequel as $\Omega(\mathbf{C}, \mathbf{X})$, namely depending on both the decoding matrix $\mathbf{C}$ and the $N_f \times 2^M$ matrix $\mathbf{X} \triangleq [\mathbf{x}_1, \cdots, \mathbf{x}_{2^M}]$ with $\mathbf{x}_i \triangleq \mathbf{b}_i \odot \mathbf{b}_i \triangleq [x_{i,0}, \cdots, x_{i,N_f-1}]^T, i \in \mathcal{I}$. Hence, after designating the $M \times 2^M$ matrix as $\mathbf{A} \triangleq [\mathbf{a}_1, \cdots, \mathbf{a}_{2^M}]$, we formulate the GCM joint constrained OP over $\mathbf{C}$ and $\mathbf{X}$, or joint OP (J-OP) for short, as

$$\begin{cases} (\mathbf{C}_o, \mathbf{X}_o) = \underset{\mathbf{C}, \mathbf{X}}{\arg\max} \{\Omega(\mathbf{C}, \mathbf{X})\} \\ \text{s.t.} \qquad \mathbf{C}^T \mathbf{X} = \Omega(\mathbf{C}, \mathbf{X}) \mathbf{A} \\ \qquad \mathbf{1}_{N_f \times 1}^T \mathbf{X} = M \mathbf{1}_{2^M \times 1}^T \\ \qquad \mathbf{X} \geq \mathbf{0}_{N_f \times 2^M} \\ \qquad \mathbf{C}^T \mathbf{1}_{N_f \times 1} = \mathbf{0}_{M \times 1} \\ \qquad \mathbf{C} \odot \mathbf{C} = \mathbf{1}_{N_f \times M} \end{cases}, \qquad (15)$$

where for convenience, we set $E_{\mathbf{b}} = M$; $\mathbf{X} \geq \mathbf{0}_{N_f \times 2^M}$ means that all entries of $\mathbf{X}$ are greater than or equal to 0; $\mathbf{C} \odot \mathbf{C} = \mathbf{1}_{N_f \times M}$ means that the entries of $\mathbf{C}$ take values in $\{\pm 1\}$; and the objective function is given by

$$\Omega(\mathbf{C}, \mathbf{X}) = \frac{1}{M2^M} \cdot \mathbf{1}_{M \times 1}^T \left[(\mathbf{C}^T \mathbf{X}) \odot \mathbf{A} \right] \mathbf{1}_{2^M \times 1}, \qquad (16)$$

which can be obtained from the first constraint of (15) originating from A3a). If the decoding matrix $\mathbf{C}$ is given, the J-OP in (15) is simplified to

$$\begin{cases} \mathbf{X}_o = \underset{\mathbf{X}}{\arg\max} \{\Omega(\mathbf{X})\} \\ \text{s.t.} \quad \mathbf{C}^T \mathbf{X} = \Omega(\mathbf{X}) \mathbf{A} \\ \qquad \mathbf{1}_{N_f \times 1}^T \mathbf{X} = M \mathbf{1}_{2^M \times 1}^T \\ \qquad \mathbf{X} \geq \mathbf{0}_{N_f \times 2^M} \end{cases}, \qquad (17)$$

labeled as GCM encoder-based OP, or E-OP for short.

Now, the following remarks about the OPs (15)-(17) are of interest.

1) The J-OP in (15) is a mixed integer programming (MIP) problem since the optimization has to be performed over the matrices $\mathbf{C}$ and $\mathbf{X}$, whose entries take integer and real values, respectively. As a result, it is generally NP-hard, and its computational complexity is really demanding even for small N_f and M. As will be shown in Sec. III-C, however, the optimal transmitted and decoding code matrices for $N_f \geq 2^M$ can be found by solving an equivalent problem for $N_f = 2^M$ with a closed-form optimal solution. In contrast, the (sub-optimal) E-OP in (17), which belongs to the class of linear programming (LP) OPs, can be solved by applying some well-known polynomial-complexity algorithms (see e.g., [25], [26]).

2) The optimal GCM design offers several advantages over the existing CM-TR and CSR: *i)* BER performance can be improved; *ii)* the system design does not rely on the properties of any codeword set, such as the Walsh codes; *iii)* the E-OP allows the optimization on any given decoding matrix satisfying A1)-A2) only; *iv)* the frame length N_f is not restricted to the form 2^N, with N being some integers, as required by the CSR; and *v)* the number of symbols M that can be embedded into a

single data block, can be greater than those of the CM-TR ($M = 1$) and the CSR ($M \leq N_f/2$), which results in a higher spectral efficiency.

3) The solutions to the J-OP or E-OP aim at optimizing the BER performance. The GCM framework gives the freedom to consider alternative optimization criteria as well. A viable option is to minimize the peak power of the transmitted signal (1) [32] under a predefined BER level determined by a value of Ω, say Ω_c, with $\Omega_c \leq \Omega_o$, Ω_o denoting the optimal objective value of J-OP in (15). This means to constrain the entries of the matrix $\mathbf{X}$ to be below a threshold Υ, or more formally $[\mathbf{X}]_{i,j} \leq \Upsilon$, $\forall j \in \mathcal{J}$, $\forall i \in \mathcal{I}$, and to modify the first constraint of (15) into $\mathbf{C}^T\mathbf{X} = \Omega_c\mathbf{A}$. Hence, the corresponding OP is to minimize the peak power Υ while keeping the average power as $\mathbf{1}_{N_f \times 1}^T\mathbf{X} = M\mathbf{1}_{2^M \times 1}^T$. Thus, this peak power based OP, or PP-OP for short, can be formulated as

$$
\begin{cases}
(\mathbf{C}_o, \mathbf{X}_o) = \underset{\mathbf{C}, \mathbf{X}}{\arg\min} \left\{ \Upsilon(\mathbf{C}, \mathbf{X}) \right\} \\
\text{s.t.} \quad \mathbf{X} \leq \Upsilon(\mathbf{C}, \mathbf{X})\mathbf{1}_{N_f \times 2^M} \\
\qquad \mathbf{C}^T\mathbf{X} = \Omega_c\mathbf{A} \\
\qquad \mathbf{1}_{N_f \times 1}^T\mathbf{X} = M\mathbf{1}_{2^M \times 1}^T \\
\qquad \mathbf{X} \geq \mathbf{0}_{N_f \times 2^M} \\
\qquad \mathbf{C}^T\mathbf{1}_{N_f \times 1} = \mathbf{0}_{M \times 1} \\
\qquad \mathbf{C} \odot \mathbf{C} = \mathbf{1}_{N_f \times M}
\end{cases}
\tag{18}
$$

4) For practical UWB communications with predetermined system parameters, i.e., N_f and M, the J-OP can be solved offline, and the optimized encoder $\chi(\mathbf{a})$ and decoding matrix $\mathbf{C} \triangleq [\mathbf{c}_1, \cdots, \mathbf{c}_M]$ can be stored locally as look-up tables at the transmitter and the receiver. When the system parameters are determined in the real-time communications, the transmitter can solve J-OP and then send the optimized decoding matrix to the receiver as preamble, or a central unit can optimize the J-OP and send the optimized results to both the transmitter and the receiver.

C. Optimal Codes for Large Frame Size N_f

The considerable complexity of the MIP constrained J-OP in (15) when $N_f > 2^M$ can be avoided by analytically solving an equivalent problem with $N_f = 2^M$. For the sake of convenience, the following two lemmas can help, where we designate the original J-OP in (15) with frame length $N_f > 2^M$ as "larger problem," or LJ-OP, and the corresponding equivalent J-OP with $N_f = 2^M$ as "smaller problem," or SJ-OP.

Lemma 1: For any feasible solution to the LJ-OP, there exists a feasible solution to the SJ-OP such that the solutions provide the same objective value Ω.

Proof: See Appendix C. ∎

Lemma 2: Assume that the mappings $\Gamma : \mathbf{A}_{2^M \times M} \to \mathbf{B}_{N_f \times M}$ and $\Lambda : \mathbf{A}_{2^M \times 2^M} \to \mathbf{B}_{N_f \times 2^M}$ exist such that for any feasible solution $(\mathbf{C}, \mathbf{X})$ to the SJ-OP, $[\Gamma(\mathbf{C}), \Lambda(\mathbf{X})]$ is the feasible solution corresponding to the LJ-OP, both with the same objective value, i.e., $\Omega(\mathbf{C}, \mathbf{X}) = \Omega[\Gamma(\mathbf{C}), \Lambda(\mathbf{X})]$. Then, $[\Gamma(\mathbf{C}_o), \Lambda(\mathbf{X}_o)]$ is the optimal solution to the LJ-OP, when $(\mathbf{C}_o, \mathbf{X}_o)$ is the optimal solution of the SJ-OP.

Proof: Corresponding to the optimal solution $(\mathbf{C}_o, \mathbf{X}_o)$ for the SJ-OP, there exists a feasible solution $[\Gamma(\mathbf{C}_o), \Lambda(\mathbf{X}_o)]$ for the LJ-OP such that $\Omega(\mathbf{C}_o, \mathbf{X}_o) = \Omega[\Gamma(\mathbf{C}_o), \Lambda(\mathbf{X}_o)] = \Omega_o$. Then, $[\Gamma(\mathbf{C}_o), \Lambda(\mathbf{X}_o)]$ must also be optimal since if there exists a solution $(\mathbf{C}', \mathbf{X}')$ to the LJ-OP which is better than $[\Gamma(\mathbf{C}_o), \Lambda(\mathbf{X}_o)]$, i.e., with $\Omega(\mathbf{C}', \mathbf{X}') > \Omega[\Gamma(\mathbf{C}_o), \Lambda(\mathbf{X}_o)]$, according to Lemma 1, there would exist a feasible solution for the SJ-OP with objective value equal to $\Omega(\mathbf{C}', \mathbf{X}')$ greater than $\Omega(\mathbf{C}_o, \mathbf{X}_o)$, which results in a contradiction. ∎

Lemmas 1 and 2 allow us to establish a one-to-one relationship between the optimal solutions of the GCM J-OPs with $N_f > 2^M$ and those with $N_f = 2^M$. Thus, the problem is how to find the mappings Γ and Λ. A simple option is to apply the zero padding method, which gives

$$
\mathbf{C}_{N_f \times M} = \Gamma_{\text{zp}}(\mathbf{C}'_{2^M \times M}) = \begin{bmatrix} \mathbf{C}'_{2^M \times M} \\ \mathbf{1}_{((N_f - 2^M)/2) \times M} \\ -\mathbf{1}_{((N_f - 2^M)/2) \times M} \end{bmatrix}, \tag{19}
$$

$$
\mathbf{X}_{N_f \times 2^M} = \Lambda_{\text{zp}}(\mathbf{X}'_{2^M \times 2^M}) = \begin{bmatrix} \mathbf{X}'_{2^M \times 2^M} \\ \mathbf{0}_{(N_f - 2^M) \times 2^M} \end{bmatrix}, \tag{20}
$$

or alternatively, the repetition codes with $N_f = P2^N$, P being a positive integer, as

$$
\mathbf{C}_{N_f \times M} = \Gamma_{\text{rc}}(\mathbf{C}'_{2^M \times M}) = \mathbf{1}_{P \times 1} \otimes \mathbf{C}'_{2^M \times M}, \tag{21}
$$

$$
\mathbf{X}_{N_f \times 2^M} = \Lambda_{\text{rc}}(\mathbf{X}'_{2^M \times 2^M}) = \frac{1}{P}\mathbf{1}_{P \times 1} \otimes \mathbf{X}'_{2^M \times 2^M}. \tag{22}
$$

It can be easily verified that $[\Gamma(\mathbf{C}), \Lambda(\mathbf{X})]$ in (19)-(22) is the feasible solution for LJ-OP, given the feasible solution $(\mathbf{C}, \mathbf{X})$ for the SJ-OP, and the solutions provide the same objective value Ω.

Now, the next step is to show that the optimal encoding and decoding matrices solving the SJ-OP can be analytically found, as stated in the sequel.

Proposition 3: Considering the GCM system with $N_f = 2^M$, the optimal decoding matrix $\mathbf{C}_o$ is the $2^M \times M$ matrix

$$
\mathbf{C}_o = [\mathbf{z}_1, \cdots, \mathbf{z}_{2^M}]^T, \tag{23}
$$

where the vectors $\mathbf{z}_i$, $i \in \mathcal{I}$, are all the 2^M realizations of length M with entries ± 1. In addition, the optimal encoder for the information symbols $\mathbf{a}$ is given by

$$
b_j = \chi_j(\mathbf{a}) = \begin{cases} \pm\sqrt{M}, & \mathbf{z}_j = \mathbf{a} \\ 0, & \text{otherwise} \end{cases}, \quad j \in \mathcal{J}, \tag{24}
$$

with the optimal objective value $\Omega_o = M$.

Proof: See Appendix D. ∎

As a further result, Lemmas 1-2 can be exploited together with Proposition 3 to derive the optimal performance of the GCM system with $N_f \geq 2^M$, as summarized in the following proposition.

Proposition 4: For a GCM system with $N_f \geq 2^M$, the optimal BER performance can be asymptotically approximated as a function of the received-bit-energy-to-noise-spectral-density ratio γ (defined after Eq. (9)) by

$$
\text{BER}_{\text{GCM}}|_{N_f \geq 2^M} = Q\left[\left(\frac{2}{\gamma M} + \frac{N_f L}{2\gamma^2 M^2}\right)^{-1/2}\right]. \tag{25}
$$

Proof: This follows from Lemmas 1-2 and Proposition 3 by plugging $\Omega_o = M$ into (9). ∎

The following remark about the optimal codes of GCM systems is now of interest.

- When $N_f = 2^M$, the optimal GCM system derived in Proposition 3 is essentially an M-PPM, and when $N_f > 2^M$, the optimal GCM system can be treated as a generalized M-PPM (e.g., PPM with zero padding or repetition in Eqs. (19)-(22)). However, different from the conventional PPM, where data symbols are carried via different delays of the transmitted pulse, the GCM systems convey the data symbols via the amplitude values of frame symbols $\mathbf{b}$, thus allowing higher data rate communications by embedding more symbols in one block, i.e., $M > \log_2(N_f)$, than the M-PPM, and enabling the system optimization with emission power constraint.

IV. CODE DESIGN FOR TRANSMISSIONS WITH IFI

This section extends the GCM framework to the case of high-rate transmissions where IFI arises when the frame interval T_f is shorter than the channel delay spread. To maintain a reasonable complexity, we will avoid an overall (constrained) optimization of the codeword matrices $\mathbf{C}$ and $\mathbf{X}$ as made in the J-OP (15) in the case of the absence of IFI. Instead, a sub-optimal yet effective IFI-mitigation method will be pursued based on a two-step procedure with a simple rationale. The basic result we will exploit can be summarized in the following lemma.

Lemma 3: Any permutation of the feasible solution $(\mathbf{C}, \mathbf{X})$ to J-OP (15), namely $(\bar{\mathbf{C}}, \bar{\mathbf{X}}) = (\mathbf{PC}, \mathbf{PX})$ with $\mathbf{P}$ being an $N_f \times N_f$ permutation matrix, is still a feasible solution satisfying all the constraints with the same objective value Ω.

Proof: From (15), it can be obtained that: *i)* $\bar{\mathbf{C}}^T \bar{\mathbf{X}} = \mathbf{C}^T \mathbf{P}^T \mathbf{PX} = \mathbf{C}^T \mathbf{X} = \Omega \mathbf{A}$; *ii)* $\mathbf{1}_{N_f \times 1}^T \bar{\mathbf{X}} = \mathbf{1}_{N_f \times 1}^T \mathbf{PX} = \mathbf{1}_{N_f \times 1}^T \mathbf{X} = M \mathbf{1}_{2^M \times 1}^T$; *iii)* $\bar{\mathbf{C}}^T \mathbf{1}_{N_f \times 1} = \mathbf{C}^T \mathbf{P}^T \mathbf{1}_{N_f \times 1} = \mathbf{C}^T \mathbf{1}_{N_f \times 1} = \mathbf{0}_{M \times 1}$; and *iv)* $\bar{\mathbf{C}} \odot \bar{\mathbf{C}} = \mathbf{C} \odot \mathbf{C} = \mathbf{1}_{N_f \times M}$. Since all the constraints are satisfied, it can be concluded that both $(\mathbf{X}, \mathbf{C})$ and $(\bar{\mathbf{C}}, \bar{\mathbf{X}}) = (\mathbf{PC}, \mathbf{PX})$ are feasible solutions to the J-OP with the same objective value Ω. ∎

Hence, in the first step of the proposed code design for transmissions with IFI, we solve J-OP (15) assuming that IFI does not exist and thus obtaining the sub-optimal solution $(\mathbf{C}_o, \mathbf{X}_o)$. Then given $(\mathbf{C}_o, \mathbf{X}_o)$, the second step consists of finding the permutation matrix $\mathbf{P}_o$ such that $(\mathbf{P}_o \mathbf{C}_o, \mathbf{P}_o \mathbf{X}_o)$ still solves J-OP (15), but at the same time, conveniently reduces the IFI contribution. Different from the J-OP, however, the optimization of the matrix $\mathbf{P}$ is now based on the reformulation of the mean value and the variance of the decision variable of Appendix A in order to account for the IFI effect as well. The aforementioned approach leads to a modified constrained OP, as stated in the following proposition.

Proposition 5: Assuming the channel template has support $[0, 2T_f]$, given the solution to J-OP (15) $(\mathbf{C}_o, \mathbf{X}_o)$, the permutation matrix $\mathbf{P}_o$, which mitigates the IFI effect in terms of BER performance, is found through the GCM IFI-based

constrained OP, or I-OP for short, formulated as

$$
\begin{cases}
\mathbf{P}_o = \arg\max_{\mathbf{P}} \{\Phi(\mathbf{P})\} \\
\text{s.t.} \quad \mathbf{C}_o^T \mathbf{P}^T \mathbf{J}_{N_f} \mathbf{PX}_o = \mathbf{A}\boldsymbol{\Phi} \\
\quad\quad \boldsymbol{\Phi} > \Phi(\mathbf{P})\mathbf{I}_{2^M} \\
\quad\quad \mathbf{P} \in \mathcal{P}
\end{cases}
\tag{26}
$$

where $\boldsymbol{\Phi} \triangleq \operatorname{diag}\{\Phi_1, \Phi_2, \cdots, \Phi_{2^M}\}$ and $\mathcal{P}$ is the set of all the permutation matrices with size $N_f \times N_f$. According to (26), the codeword matrices to be employed for IFI mitigation become $(\mathbf{P}_o \mathbf{C}_o, \mathbf{P}_o \mathbf{X}_o)$.

Proof: See Appendix E. ∎

A few remarks about Proposition 5 can be made as follows.

1) As shown in Appendix E, the OP (26) relies on maximizing a part of the mean value of the decision variable that corresponds to the contribution of interfering symbols. Therefore, the optimal permutation matrix $\mathbf{P}_o$ can be interpreted as an "equalization" matrix such that the frame energy from the previous symbol can be properly exploited within the current frame.

2) Unlike J-OP (15) where the constraint $\mathbf{C}^T \mathbf{X} = \Omega(\mathbf{C}, \mathbf{X})\mathbf{A}$ holds with the scalar Ω, in I-OP (26), this restriction is circumvented by adopting the diagonal matrix $\boldsymbol{\Phi}$ and adding the constraint $\boldsymbol{\Phi} > \Phi(\mathbf{P})\mathbf{I}_{2^M}$. After all, with only a scalar as in (15), there may not exist a feasible $\mathbf{P}$ given $(\mathbf{C}_o, \mathbf{X}_o)$ such that all 2^M equalities can hold. Furthermore, although the aforementioned choice yields better performance, as demonstrated in Sec. V, the BER for different realization $\mathbf{a}_i$ of the information symbols may differ.

V. NUMERICAL RESULTS

In this section, we illustrate the optimal solutions of the proposed OPs for some values of the number of frames N_f and the number of symbols M per block. Then, the performance of the proposed optimal GCM systems is quantified through numerical simulations, taking as benchmark the existing CSR design in [22] using Walsh codes. We do not consider the FSR system, which shows identical performance to the CM-TR systems in the absence of IFI and inferior performance in the presence of IFI [21], [22]. The transmitted pulse $p(t)$ is the second derivative of a Gaussian function with width $T_p = 1.0$ ns. We use the channel models described in [23] for random channel realizations. The one-sided bandwidth of the low-pass filter at the receiver is $B = 2.5$ GHz. In this section, all OPs are solved using the general solver in [27].

A. Optimal Codes for GCM Systems

Table I summarizes the optimization results of J-OP (15) corresponding to the number of frames $N_f = 2, 4, 6, 8$ and a few values of the number of symbols M conveyed by each block. When $(N_f = 2, M = 1)$, $(N_f = 4, M = 1)$, $(N_f = 8, M = 1)$, and $(N_f = 8, M = 4)$, the proposed codes offer the same performance as the CSR systems using Walsh codes, which means that Walsh codes are optimal for these cases. On the other hand, when $(N_f = 4, M = 2)$, $(N_f = 8, M = 2)$, and $(N_f = 8, M = 3)$, since the CSR systems using

Walsh codes yield sub-optimal solutions to the OP in (15), i.e., the CSR systems are not optimized in the view of power efficiency, the proposed codes achieve significant improvement compared to the CSR systems. Additionally, the optimization performed on $(N_f = 4, M = 3)$ and $N_f = 6$, where Walsh codes do not exist, gives us the flexibility to design GCM systems with different N_f and M. Finally, the results for $N_f \geq 2^M$ corroborate Proposition 4, where $\Omega_o = M$.

Frame length	Number of symbols	Walsh codes	Optimal codes
$N_f = 2$	$M = 1$	1	1
$N_f = 4$	$M = 1$	1	1
	$M = 2$	$\sqrt{2}$	2
	$M = 3$	N/A	1
$N_f = 6$	$M = 1$	N/A	1
	$M = 2$	N/A	2
	$M = 3$	N/A	1
$N_f = 8$	$M = 1$	1	1
	$M = 2$	$\sqrt{2}$	2
	$M = 3$	$\sqrt{3}$	3
	$M = 4$	2	2

TABLE I
OBJECTIVE VALUE Ω FOR THE CSR WITH WALSH CODES AND THE GCM WITH OPTIMAL CODES.

B. Performance of Optimal Codes for GCM Systems

Fig. 2 displays the BER performance of the proposed GCM systems for $N_f = 4, 8$ and different numbers of information symbols per block M. We adopt CM1 channel model with $T_f = 80$ ns to avoid IFI and $L = 2BT_f = 400$. Given N_f and M, it is worth noting that the theoretical BERs in (9) overlap with the simulated curves. This result validates the accuracy of the Gaussian approximation whenever L is large which we assumed in the proof of Proposition 1. In all, the system with $(N_f = 8, M = 3)$ achieves the best BER performance and gains about 1.8 dB over the $(N_f = 8, M = 2)$ one at BER $= 10^{-5}$. When $N_f = 4$, the optimal system with $M = 2$ is close to that with $(N_f = 8, M = 3)$, while outperforms the $(N_f = 4, M = 1)$ one by about 3 dB at BER$= 10^{-5}$.
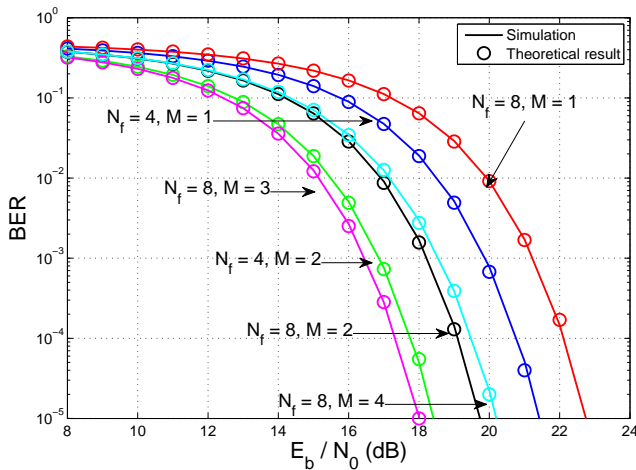

Fig. 2.   BER performance of the optimal GCM with different frame sizes N_f and number of symbols M.

C. Performance Comparisons of Optimal GCM Systems with Existing Design

In this subsection, we compare the performance of the GCM systems with optimal codes to the CSR system in [22] and simple TR (STR) system in [11] with CM1 channel model and $T_f = 80$ ns. Fig. 3 verifies the BER improvement of the proposed GCM over the existing designs. At BER$= 10^{-5}$, indeed, for the cases of $(N_f = 4, M = 2)$ and $(N_f = 8, M = 2)$ the proposed GCM design outperforms the CSR by about 1.8 dB, whereas for $(N_f = 8, M = 3)$ case, the advantage of the optimal system increases to about 2.7 dB.
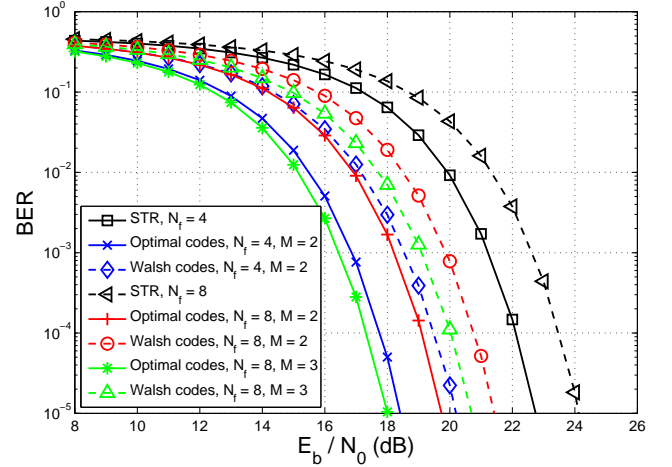

Fig. 3.   BER comparisons for the GCM using optimal codes, the design in [22] using Walsh codes, and the STR.

D. GCM Systems with Peak-to-Average Power Ratio Constraint

Fig. 4 depicts the relationship between the peak-to-average power ratio (PAPR) which is defined as

$$\text{PAPR} = \frac{\max X_{j,i}}{\left(\sum_{i=1}^{2^M} \sum_{j=0}^{N_f-1} X_{j,i}/2^M/N_f\right)}, \quad (27)$$

and Ω_c of the GCM systems with $N_f = 8$ and different M. Here, we compare PAPRs of the GCM systems optimized by PP-OP (18) for different levels of Ω_c, $\Omega_c \leq \Omega_o$ and the Walsh code. Note that, for $M = 2, 4$, since $\Omega_o = 2$, we only have the results for $\Omega_c \leq 2$. For GCM system in J-OP (15), PAPR becomes $\max X_{j,i} N_f/M$ since we assumed that $\mathbf{1}_{N_f \times 1}^T \mathbf{X} = M\mathbf{1}_{2^M \times 1}^T$. From Fig. 4, first of all, as Ω_c increases (therefore, with better error performance), the minimum PAPR increases monotonically, thus providing the trade-off between the system error performance and the PAPR value. Secondly, the PAPRs of $M = 2$ and $M = 4$ are the same when $\Omega_c = 0.5, 1, 1.5, 2$ and their PAPRs are higher than those of $M = 3$ when $\Omega_c = 0.5, 1, 1.5$. Thus, unlike the case of Ω_c, the PAPR is not a monotonically increasing or decreasing function depending on M. Thirdly, the GCM system optimized by PP-OP (18) yields smaller PAPR than the CSR system with the Walsh code thus confirming effectiveness of our GCM code design.
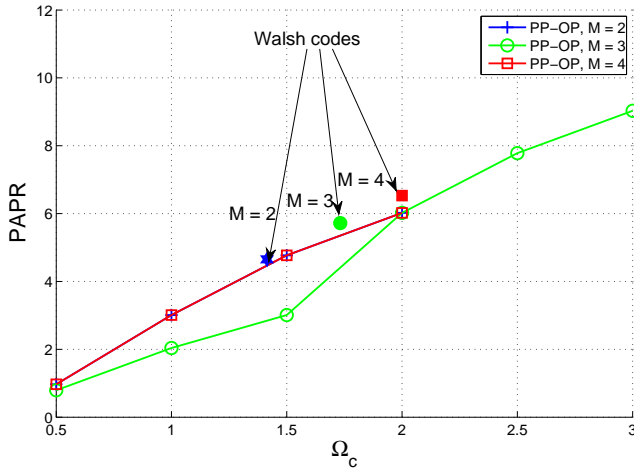
Fig. 4. Peak-to-average power ratio for different GCM systems with $N_f = 8$.

Fig. 5. BER comparisons for different GCM systems with and without optimal code sequence design in the presence of IFI with CM1 channel.

E. Performance Comparisons of GCM with IFI

Fig. 5 illustrates the BER comparisons with CM1 channel model and the following code-multiplexing systems: *i)* GCM system with optimal solution from J-OP (15) and optimal code sequence design from I-OP (26), *ii)* GCM system with optimal solution from J-OP (15) but with non-optimal code sequence design, and *iii)* CSR with Walsh code. $N_f = 8$ and $M = 2$. For *i)* and *ii)*, we firstly obtain the transmitted symbols matrix and decoding matrix from J-OP (15) as:

$$\mathbf{X}_o = \begin{bmatrix} 1 & 0 & 1 & 0 & 0 & 0 & 0 & 0 \\ 0 & 1 & 0 & 1 & 0 & 0 & 0 & 0 \\ 0 & 0 & 0 & 0 & 1 & 0 & 1 & 0 \\ 0 & 0 & 0 & 0 & 0 & 1 & 0 & 1 \end{bmatrix}^T, \qquad (28)$$

$$\mathbf{C}_o = \begin{bmatrix} +1 & +1 & +1 & +1 & -1 & -1 & -1 & -1 \\ +1 & -1 & +1 & -1 & +1 & -1 & +1 & -1 \end{bmatrix}^T, \qquad (29)$$

with $\Omega_o = 2$. Next, we solve I-OP (26) with $(\mathbf{C}_o, \mathbf{X}_o)$ in Eqs. (28) and (29) and the optimal permutation matrix is

$$\mathbf{P}_o = \begin{bmatrix} \mathbf{e}_1 & \mathbf{e}_3 & \mathbf{e}_2 & \mathbf{e}_4 & \mathbf{e}_5 & \mathbf{e}_7 & \mathbf{e}_6 & \mathbf{e}_8 \end{bmatrix}, \qquad (30)$$

where $\mathbf{e}_j$ denotes the jth column of an identity matrix $\mathbf{I}_{N_f}$. Therefore, the corresponding codewords for *i)* are $\bar{\mathbf{X}}_o = \mathbf{P}_o \mathbf{X}_o$, $\bar{\mathbf{C}}_o = \mathbf{P}_o \mathbf{C}_o$ with $\Phi_o = 0$ and we adopt $(\mathbf{C}_o, \mathbf{X}_o)$ in Eqs. (28) and (29) for *ii)* with $\Phi = -1$.

To simulate a high-rate UWB communication in a stringent channel environment, we set $T_f = 6, 8$ ns to include IFI and data rate 41.67 Mbit/s and 31.25 Mbit/s, respectively. As shown in Fig. 5, when $T_f = 8$ ns, the GCM with optimal code sequence design achieves 1 dB gain over the one with non-optimal sequence design and 4 dB gain over the CSR system with Walsh code at BER = 10^{-5}. When the data rate increases ($T_f = 6$ ns), the advantage of the optimal code sequence design is clear and the gap between optimal sequence and non-optimal code sequence increases to around 10 dB at BER = 2×10^{-2}.

In addition, we compare the BER performance of different code-multiplexing systems with CM4 channel model, whose maximum excess delay T_m is about 360 ns. Due to the long
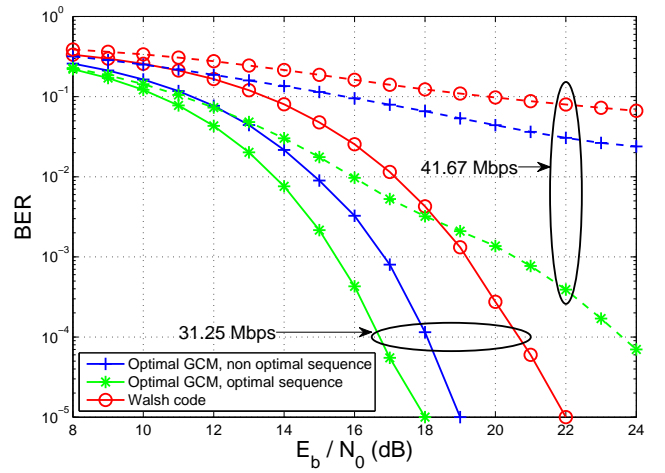
excess delay, the frame duration T_f is increased to 30 or 40 ns in order to obtain affordable system performance. From Fig. 6, similar conclusions about the results for the CM1 channel model can be drawn for the CM4 one as well. In fact, the optimal GCM system with optimal code sequence design obtains the best error performance among the three systems and the gains relative to non-optimal code sequence design become around 1.5 dB and 5 dB for $T_f = 30, 40$ ns, respectively, at BER = 10^{-5}.
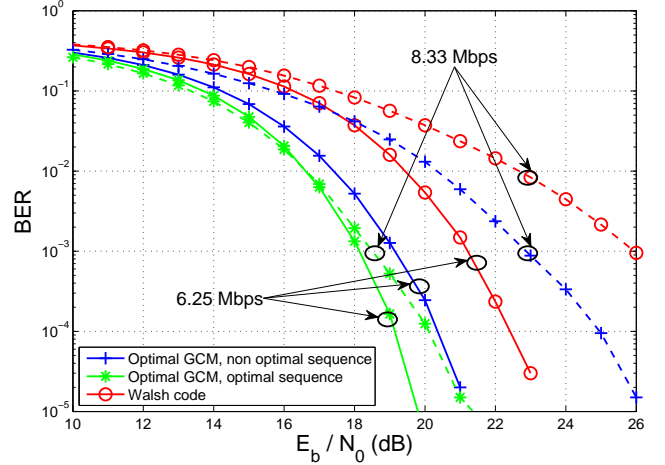

Fig. 6. BER comparisons for different GCM systems with and without optimal code sequence design in the presence of IFI with CM4 channel.

VI. CONCLUSION

In this paper, we have proposed a GCM system that extends and outperforms the existing CM-TR and CSR schemes. We have formulated a constrained optimization problem with the aim of maximizing the BER link performance, whose complexity can be mitigated by considering an equivalent system with a shorter frame size. Simulations over demanding propagation environments corroborate the competitiveness of the proposed approach. Furthermore, we have studied the

GCM optimization with emission power constraint and generalized the GCM optimization problem to situations when moderate IFI may occur, with the result of gaining improved BER performance over the existing Walsh-code based design.

APPENDIX A: PROOF OF PROPOSITION 1

We prove that assumption A3) is equivalent to A3a)-A3b), assuming the absence of IFI and a sufficiently large product BT_f, i.e., between the bandwidth B of the receiver low-pass filter $h_{\mathrm{LP}}(t)$ and the frame interval T_f. First, let us focus on the statistics of the samples at the integrator output $r_j, j \in \mathcal{J}$, given by (4). Exploiting the IFI-free condition, i.e., that the support of the channel template $g(t)$ is less than the frame interval T_f, and keeping in mind the expression of the received signal in (3), we obtain

$$r_j = b_j^2 \int_0^{T_f} g^2(t)dt + \underbrace{2b_j \int_0^{T_f} g(t)w_j(t)dt + \int_0^{T_f} w_j^2(t)\, dt}_{\varphi_j},$$
(31)

where $w_j(t) \triangleq w(t + jT_f)$.

Applying the sampling theorem to the (31) yields (c.f., [24])

$$r_j = b_j^2 E_f + \underbrace{2b_j \sum_{n=0}^{L-1} w_{j,n} g_n}_{\varphi_{j,1}} + \underbrace{\sum_{n=0}^{L-1} w_{j,n}^2}_{\varphi_{j,2}},$$
(32)

where $L \triangleq \lceil 2BT_f \rceil$, $g_n \triangleq \sqrt{T_s}g(nT_s)$, $w_{j,n} \triangleq \sqrt{T_s}w_j(nT_s)$ are independent and identically distributed (i.i.d.) Gaussian random variables with zero mean and variance $N_0/2$, $T_s \triangleq \frac{1}{2B}$ is the sampling interval, and $E_f = \sum_{n=0}^{L-1} g_n^2$. If L is sufficiently large, in view of the central limit theorem, $\varphi_{j,2}$ can be approximated as a Gaussian random variable. Since $\mathrm{E}\{\varphi_{j,1}\varphi_{j,2}\} = \mathrm{E}\{\sum_{n=0}^{L-1} g_n w_{j,n}^3\} = 0$, we can treat $\varphi_{j,1}$ and $\varphi_{j,2}$ as independent Gaussian-distributed variables. Therefore, the mean and the variance of r_j for a given realization of the symbols $\mathbf{a}$ are given, respectively, by [21], [22], [24]

$$\mathrm{E}\{r_j|\mathbf{a}\} = b_j^2 E_f + \frac{LN_0}{2},$$
(33)

$$\begin{aligned}
\mathrm{Var}\{r_j|\mathbf{a}\} &= \mathrm{Var}\{\varphi_j|\mathbf{a}\} \\
&= \mathrm{Var}\{\varphi_{j,1}|\mathbf{a}\} + \mathrm{Var}\{\varphi_{j,2}|\mathbf{a}\} \\
&= 4b_j^2 \sum_{n=0}^{L-1} g_n^2 \mathrm{Var}\{w_{j,n}\} + \sum_{n=0}^{L-1} \left(\mathrm{E}\{w_{j,n}^4\} - \mathrm{E}\{w_{j,n}^2\}^2 \right) \\
&= 2b_j^2 E_f N_0 + \frac{LN_0^2}{2}.
\end{aligned}$$
(34)

Therefore, the decision variable $z_k, k \in \mathcal{K}$, in (5) can be rearranged as

$$z_k = \mathbf{c}_k^T \mathbf{r} = E_f \mathbf{c}_k^T (\mathbf{b} \odot \mathbf{b}) + \xi_k,$$
(35)

where, under assumptions A1)-A2) of Definition 1, $\xi_k \triangleq \mathbf{c}_k^T \boldsymbol{\varphi}$, with $\boldsymbol{\varphi} \triangleq \left[\varphi_0, \cdots, \varphi_{N_f-1}\right]^T$, has mean

$$\mathrm{E}\{\xi_k|\mathbf{a}\} = \frac{LN_0}{2} \sum_{j=0}^{N_f-1} c_{k,j} = 0,$$
(36)

and variance

$$\mathrm{Var}\{\xi_k|\mathbf{a}\} = 2E_f N_0 \sum_{j=0}^{N_f-1} b_j^2 + \frac{N_f LN_0^2}{2}.$$
(37)

Hence, z_k in (35) can be modeled for a given vector $\mathbf{a}$ as a Gaussian-distributed random variable, whose mean and variance after imposing assumptions A3a)-A3b) and (35)-(36) are given by

$$\mathrm{E}\{z_k|\mathbf{a}\} = E_f \mathbf{c}_k^T (\mathbf{b} \odot \mathbf{b}) = E_f \Psi\, a_{i,k}, i \in \mathcal{I}, k \in \mathcal{K},$$
(38)

and

$$\mathrm{Var}\{z_k|\mathbf{a}\} = 2E_f N_0 E_{\mathbf{b}} + \frac{N_f LN_0^2}{2},$$
(39)

respectively. Therefore, we deduce from (38)-(39) that the error probabilities on $a_k, k \in \mathcal{K}$, are all the same. Similarly, it can be shown that assumption A3) induces A3a)-A3b), which concludes the proof about the necessary and sufficient condition of assumption A3).

APPENDIX B: PROOF OF PROPOSITION 2

Due to assumption A3b), i.e., $\|\mathbf{b}_i\|_2^2 = E_{\mathbf{b}}, i \in \mathcal{I}$, the received bit energy results in

$$E_{bit} = \frac{E_f}{M} \sum_{j=0}^{N_f-1} b_j^2 = \frac{E_f}{M} E_{\mathbf{b}}.$$
(40)

Hence, from (38)-(39), the error probabilities on the information symbols a_k become identical over k and are expressed by

$$\begin{aligned}
\mathrm{BER}_{\mathrm{GCM}}(\Omega) &= Q\left[\left(\frac{\mathrm{E}\{z_k|\mathbf{a}\}^2}{\mathrm{Var}\{z_k|\mathbf{a}\}} \right)^{1/2} \right] \\
&= Q\left[\left(\frac{E_f^2 \Psi^2}{2E_f N_0 E_{\mathbf{b}} + N_f LN_0^2/2} \right)^{1/2} \right] \\
&= Q\left[\left(\frac{2E_f N_0 E_{\mathbf{b}} + N_f LN_0^2/2}{E_f^2 \Psi^2} \right)^{-1/2} \right] \\
&= Q\left[\left(\frac{E_{\mathbf{b}}^2}{\Psi^2 M^2} \left(\frac{2MN_0}{E_{bit}} + \frac{N_f LN_0^2}{2E_{bit}^2} \right) \right)^{-1/2} \right] \\
&= Q\left[\Omega \left(\frac{2M}{\gamma} + \frac{N_f L}{2\gamma^2} \right)^{-1/2} \right],
\end{aligned}$$
(41)

where $\gamma \triangleq E_{bit}/N_0$ and $\Omega \triangleq M\Psi/E_{\mathbf{b}}$.

APPENDIX C: PROOF OF LEMMA 1

The feasible solution $\mathbf{C}$ for the J-OP (15) is an $N_f \times M$ matrix, which has, at most, 2^M distinct rows due to assumption A1). Hence, a $2^M \times M$ decoding matrix $\bar{\mathbf{C}}$ can be constructed whose rows are all the 2^M realizations with entries $\{\pm 1\}$ such that

$$\mathbf{C} = \mathbf{T}\bar{\mathbf{C}},$$
(42)

where $\mathbf{T}$ is an $N_f \times 2^M$ mapping matrix having in each row only one element equal to 1 and all the others equal to 0. It can be obtained

$$\mathbf{1}_{2^M \times 1}^T \mathbf{T}^T \mathbf{X} = \mathbf{1}_{N_f \times 1}^T \mathbf{X} = M \mathbf{1}_{2^M \times 1}^T, \qquad (43)$$

$$\bar{\mathbf{C}}^T \bar{\mathbf{X}} = \bar{\mathbf{C}}^T \mathbf{T}^T \mathbf{X} = (\mathbf{T}\bar{\mathbf{C}})^T \mathbf{X} = \mathbf{C}^T \mathbf{X}, \qquad (44)$$

i.e., the matrices $\bar{\mathbf{C}}$ and $\bar{\mathbf{X}} \triangleq \mathbf{T}^T \mathbf{X}$ satisfy both the first and second constraints of the J-OP as well. Since $\bar{\mathbf{C}}^T \mathbf{1}_{2^M \times 1} = \mathbf{0}_{M \times 1}$ and $\bar{\mathbf{C}} \odot \bar{\mathbf{C}} = \mathbf{1}_{2^M \times M}$, we conclude that $(\bar{\mathbf{C}}, \bar{\mathbf{X}}) = (\bar{\mathbf{C}}, \mathbf{T}^T \mathbf{X})$ is a feasible solution to the J-OP (15) with $N_f = 2^M$ (SJ-OP) and the value of the objective function is the same as that given by the feasible solution $(\mathbf{C}, \mathbf{X})$ with $N_f > 2^M$ (LJ-OP).

APPENDIX D: PROOF OF PROPOSITION 3

Bearing in mind the proof of Lemma 1, the optimal decoding matrix $\mathbf{C}_o$ for the GCM system with frame length $N_f = 2^M$ is known to be the $2^M \times M$ matrix given by (23), with the rows being all the realizations of length M with entries ± 1. Hence, the J-OP in (15) can be relaxed to the set of 2^M decoupled OPs

$$\begin{cases} \mathbf{x}_i^{(o)} = \arg\max_{\mathbf{x}_i} \{\Omega_i(\mathbf{x}_i)\} \\ \text{s.t.} \quad \mathbf{a}_i^T \mathbf{a}_i \Omega_i(\mathbf{x}_i) = (\mathbf{C}_o \mathbf{a}_i)^T \mathbf{x}_i \\ \qquad \mathbf{1}_{2^M \times 1}^T \mathbf{x}_i = M \\ \qquad \mathbf{x}_i \geq \mathbf{0}_{2^M \times 1} \end{cases} \qquad (45)$$

each corresponding to a different realization $\mathbf{a}_i$ of the information symbols.

It is readily shown that, the optimal solution of the OP (45) is

$$x_{i,j}^{(o)} = \begin{cases} M, & j = \bar{k} \\ 0, & \text{otherwise} \end{cases}, \quad i,j \in \mathcal{I}, \qquad (46)$$

where $\bar{k} = \arg\max_k [\mathbf{C}_o \mathbf{a}_i]_k$, i.e., $\mathbf{z}_{\bar{k}} = \mathbf{a}_i$. Now, we note that: i) since $\mathbf{x}_i^{(o)}$ in (46) is the feasible solution of OP (45), then it optimally solves also (45); ii) the optimal values of Ω_i concerning the 2^M OPs in (45) are all equal to M. Therefore, it can be concluded that $\mathbf{X}_o \triangleq [\mathbf{x}_1^{(o)}, \cdots, \mathbf{x}_{2^M}^{(o)}]$ is the optimal solution of the J-OP (15).

APPENDIX E: PROOF OF PROPOSITION 5

Assume that the channel template can be written as $g(t) = g_0(t) + g_1(t - T_f)$, with both $g_0(t)$ and $g_1(t)$ having support $[0, T_f]$. Similar to the approach used in Appendix A, in view of large $L = \lceil 2BT_f \rceil$, the mean value and the variance of r_j for a given realization of the information symbols $\mathbf{a}$ can be written as

$$E\{r_j|\mathbf{a}\} = b_j^2 E_f^{(0)} + b_{j-1}^2 E_f^{(1)} + 2b_j b_{j-1} E_f^{(0,1)} + \frac{LN_0}{2}, \qquad (47)$$

$$\text{Var}\{r_j|\mathbf{a}\} = 2\left(b_j^2 E_f^{(0)} + b_{j-1}^2 E_f^{(1)} + 2b_j b_{j-1} E_f^{(0,1)}\right)N_0 + \frac{LN_0^2}{2}, \qquad (48)$$

where $E_f^{(0)} = \int_0^{T_f} g_0^2(t)dt$, $E_f^{(1)} = \int_0^{T_f} g_1^2(t)dt$, and $E_f^{(0,1)} = \int_0^{T_f} g_1(t)g_2(t)dt$. Then, assuming $E_f^{(0,1)} \ll E_f^{(0)}$ and $E_f^{(0,1)} \ll E_f^{(1)}$ [21], (47)-(48) can be approximated as

$$E\{r_j|\mathbf{a}\} \approx b_j^2 E_f^{(0)} + b_{j-1}^2 E_f^{(1)} + \frac{LN_0}{2}, \qquad (49)$$

$$\text{Var}\{r_j|\mathbf{a}\} \approx 2\left(b_j^2 E_f^{(0)} + b_{j-1}^2 E_f^{(1)}\right)N_0 + \frac{LN_0^2}{2}. \qquad (50)$$

Now, by applying the $N_f \times N_f$ permutation matrix $\mathbf{P}$ on the solution $(\mathbf{C}_o, \mathbf{X}_o)$ to J-OP (15), one obtains the feasible solution $(\bar{\mathbf{C}}, \bar{\mathbf{X}}) = (\mathbf{P}\mathbf{C}_o, \mathbf{P}\mathbf{X}_o)$. Accordingly, the mean value and the variance of the decision variable $z_k = \sum_{j=0}^{N_f-1} \bar{c}_{j,k} r_j$, for a given $\mathbf{a}_i$, result as

$$E\{z_k|\mathbf{a}_i\} \approx \sum_{j=0}^{N_f-1} \bar{c}_{j,k} \left[E_f^{(0)} \bar{b}_{j,i}^2 + E_f^{(1)} \bar{b}_{j-1,i}^2\right], \qquad (51)$$

$$\text{Var}\{z_k|\mathbf{a}_i\} \approx 2N_0 E_f \sum_{j=0}^{N_f-1} \bar{b}_{j,i}^2 + \frac{N_f L N_0^2}{2}, \qquad (52)$$

where $\bar{c}_{j,k} \triangleq [\bar{\mathbf{C}}]_{j,k}$ and $\bar{b}_{j,i}^2 \triangleq [\bar{\mathbf{X}}]_{j,i}$, $j \in \mathcal{J}$, $i \in \mathcal{I}$, $1 \leq k \leq M$. Since Lemma 3 shows that both $(\mathbf{C}_o, \mathbf{X}_o)$ and $(\bar{\mathbf{C}}, \bar{\mathbf{X}})$ satisfy all constraints of the J-OP (15) with the same objective Ω, we have: i) $\sum_{j=0}^{N_f-1} \bar{c}_{j,k} \bar{b}_{j,i}^2 = \Omega a_{i,k}$, and ii) $\sum_{j=0}^{N_f-1} \bar{b}_{j,i}^2 = M$, $\forall i \in \mathcal{I}$. This means that (51)-(52) turn into

$$E\{z_k|\mathbf{a}_i\} \approx E_f^{(0)} \Omega a_{i,k} + E_f^{(1)} \sum_{j=0}^{N_f-1} \bar{c}_{j,k} \bar{b}_{j-1,i}^2, \qquad (53)$$

$$\text{Var}\{z_k|\mathbf{a}_i\} \approx 2N_0 E_f M + \frac{N_f L N_0^2}{2}, \qquad (54)$$

respectively. Bearing in mind that the variance in (54) is independent of both $\bar{\mathbf{C}}$ and $\bar{\mathbf{X}}$, we can argue from (53) that a possible criterion to mitigate IFI in terms of BER performance is to choose the permutation matrix $\mathbf{P}$ such that the constraints

$$\sum_{j=0}^{N_f-1} \bar{c}_{j,k} \bar{b}_{j-1,i}^2 = \Phi_i a_{i,k}, \quad i \in \mathcal{I}, \qquad (55)$$

hold. After dropping the terms $\bar{b}_{-1,i}^2$ caused by inter-block interference (IBI), (55) can be equivalently put in matrix notation as

$$\mathbf{C}_o^T \mathbf{P}^T \mathbf{J}_{N_f} \mathbf{P} \mathbf{X}_o = \mathbf{A}\mathbf{\Phi}, \qquad (56)$$

where $\mathbf{\Phi} \triangleq \text{diag}\{\Phi_1, \Phi_2, \cdots, \Phi_{2^M}\}$ and $\mathbf{A}$ is the $M \times 2^M$ matrix containing all the realizations $\mathbf{a}_i$. Then, we add the constraints

$$\mathbf{\Phi} > \Phi \mathbf{I}_{2^M}, \qquad (57)$$

and maximize Φ to have a scalar-valued objective function.

In summary, the matrices for IFI mitigation will result as $(\mathbf{P}_o \mathbf{C}_o, \mathbf{P}_o \mathbf{X}_o)$, where the optimal permutation matrix $\mathbf{P}_o$ is found by maximizing the scalar objective Φ under the constraints (56)-(57).

## REFERENCES

[1] M. Z. Win and R. A. Scholtz, "Impulse radio: how it works," *IEEE Commun. Lett.*, vol. 2, no. 2, pp. 36–38, Feb. 1998.

[2] L. Yang and G. B. Giannakis, "Ultra-wideband communications: an idea whose time has come," *IEEE Signal Process. Mag.*, vol. 21, no. 6, pp. 26–54, Nov. 2004.

[3] K. Witrisal, G. Leus, G. Janssen, M. Pausini, F. Troesch, T. Zasowski, and J. Romme, "Noncoherent ultra-wideband systems," *IEEE Signal Process. Mag.*, vol. 26, no. 4, pp. 48–66, Jul. 2009.

[4] R. J. M. Cramer, R. A. Scholtz, and M. Z. Win, "Evaluation of an ultra-wideband propagation channel," *IEEE Trans. Antennas Propag.*, vol. 50, no. 5, pp. 561–570, May 2002.

[5] M. Z. Win and R. A. Scholtz, "Characterization of ultra-wide bandwidth wireless indoor channels: a communication-theoretic view," *IEEE J. Sel. Areas Commun.*, vol. 20, no. 9, pp. 1613–1627, Dec. 2002.

[6] D. Cassioli, M. Z. Win, and A. F. Molisch, "The ultra-wide bandwidth indoor channel: from statistical model to simulations," *IEEE J. Sel. Areas Commun.*, vol. 20, no. 6, pp. 1247–1257, Aug. 2002.

[7] D. Cassioli, F. Vatalaro, M. Z. Win, and A. F. Molisch, "Performance of low-complexity rake reception in a realistic UWB channel," in *Proc.IEEE Int. Conf. Commun.*, vol. 2, May 2002, pp. 763–767.

[8] J. D. Choi and W. E. Stark, "Performance of ultra-wideband communications with suboptimal receivers in multipath channels," *IEEE J. Sel. Areas Commun.*, vol. 20, no. 9, pp. 1754–1766, Dec. 2002.

[9] V. Lottici, A. D'Andrea, and U. Mengali, "Channel estimation for ultra-wideband communications," *IEEE J. Sel. Areas Commun.*, vol. 20, no. 9, pp. 1638–1645, Dec. 2002.

[10] R. Hoctor and H. Tomlinson, "Delay-hopped transmitted-reference RF communications," in *Proc. IEEE UWBST*, May 2002, pp. 265–269.

[11] Y.-L. Chao and R. A. Scholtz, "Optimal and suboptimal receivers for ultra-wideband transmitted reference systems," in *Proc. IEEE Globecom*, vol. 2, Dec. 2003, pp. 759–763.

[12] T. Q. S. Quek and M. Z. Win, "Analysis of UWB transmitted-reference communication systems in dense multipath channels," *IEEE J. Sel. Areas Commun.*, vol. 23, no. 9, pp. 1863–1874, Sep. 2005.

[13] L. Yang and G. B. Giannakis, "Optimal pilot waveform assisted modulation for ultrawideband communications," *IEEE Trans. Wireless Commun.*, vol. 3, no. 4, pp. 1236–1249, Jul. 2004.

[14] N. van Stralen, A. Dentinger, I. Welles, K. J. Gaus, R., R. Hoctor, and H. Tomlinson, "Delay hopped transmitted reference experimental results," in *Proc. IEEE UWBST*, May 2002, pp. 93–98.

[15] L. Feng and W. Namgoong, "An oversampled channelized UWB receiver with transmitted reference modulation," *IEEE Trans. Wireless Commun.*, vol. 5, no. 6, pp. 1497–1505, Jun. 2006.

[16] M. Casu and G. Durisi, "Implementation aspects of a transmitted-reference UWB receiver," *Wireless Commun. and Mobile Comput.*, vol. 5, no. 5, pp. 537–549, May 2005.

[17] M. Ho, V. S. Somayazulu, J. Foerster, and S. Roy, "A differential detector for an ultra-wideband communications system," in *Proc. IEEE VTC*, vol. 4, May 2002, pp. 1896–1900.

[18] V. Lottici and Z. Tian, "Multiple symbol differential detection for UWB communications," *IEEE Trans. Wireless Commun.*, vol. 7, no. 5, pp. 1656–1666, May 2008.

[19] Q. Zhou, X. Ma, and V. Lottici, "Fast multi-symbol based iterative detectors for UWB communications," *EURASIP J. Appl. Signal Process.*, vol. 2010, May 2010.

[20] D. L. Goeckel and Q. Zhang, "Slightly frequency-shifted reference ultra-wideband (UWB) radio," *IEEE Trans. Commun.*, vol. 55, no. 3, pp. 508–519, Mar. 2007.

[21] A. A. D'amico and U. Mengali, "Code-multiplexed UWB transmitted-reference radio," *IEEE Trans. Commun.*, vol. 56, no. 12, pp. 2125–2132, Dec. 2008.

[22] H. Nie and Z. Chen, "Code-shifted reference transceiver for impulse radio ultra-wideband systems," *Physical Commun.*, vol. 2, pp. 274–284, Dec. 2009.

[23] J. R. Foerster, *Channel Modeling Sub-committee Report Final*, IEEE P802.15-02/368r5-SG3a Std., 2002.

[24] H. Urkowitz, "Energy detection of unknown deterministic signals," *Proc. IEEE*, vol. 55, no. 4, pp. 523–531, Apr. 1967.

[25] N. Karmarkar, "A new polynomial-time algorithm for linear programming," in *Proc. 16th Annual ACM Symp. on Theory of Computing*, New York, NY, USA, pp. 302–311.

[26] S. P. Boyd and L. Vandenberghe, *Convex optimization*. Cambridge Univ. Pr., 2004.

[27] L. S. Inc., "LINGO - Optimization Modeling Software for Linear, Nonlinear, and Integer Programming," http://www.lindo.com.

[28] Q. Zhang and C. Ng, "Differentially-encoded di-symbol time-division multiuser impulse radio in UWB channel," *IEEE Trans. Commun.* vol. 56, no. 4, pp. 608–618, Apr. 2008.

[29] Q. Zhang and A. Nallanathan, "Transmitted-reference impulse radio systems based on selective combining," *IEEE Trans. Wireless Commun.*, vol. 7, no. 11, pp. 4105–4109, Nov. 2008.

[30] Q. Zhang, H. K. Garg, and A. Nallanathan, "Monobit digital eigen-based receiver for transmitted-reference UWB communications," *IEEE Trans. Wireless Commun.*, vol. 8, no. 5, pp. 2312–2316, May 2009.

[31] M. Tutay and S. Gezici, "Optimal and suboptimal receivers for code-multiplexed transmitted-reference ultra-wideband systems," *Wireless Commun. and Mobile Comput.*, Sep. 2011, doi: 10.1002/wcm.1191.

[32] C. Abou-Rjeily, N. Daniele, and J. Belfiore, "On the amplify-and-forward cooperative diversity with time-hopping ultra-wideband communications," *IEEE Trans. Commun.*, vol. 56, no. 4, pp. 630–641, Apr. 2008.

Qi Zhou (S'10) received the B.S. degree in Mathematics and Applied Mathematics from the Beijing University of Posts and Telecommunications, Beijing, P. R. China, in 2006, the M.S. degree in Computer Science from Shanghai Jiaotong University, Shanghai, P. R. China, in 2009, and the M.S. degree in Electrical and Computer Engineering from the Georgia Institute of Technology, Atlanta, GA, in 2009. He is now working towards the Ph.D. degree in the School of Electrical and Computer Engineering, Georgia Institute of Technology. His current research interests include transceiver designs for ultra-wideband communications, interference mitigation for femtocell/macrocell networks, equalizations for large multiple-input multiple-output systems, and VLSI implementation of energy-efficient high-throughput detectors.
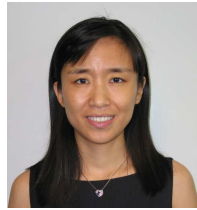
Xiaoli Ma (SM'09) received the B.S. degree in automatic control from Tsinghua University, Beijing, China in 1998, the M.S. degree in electrical engineering from the University of Virginia, Charlottesville, in 2000, and the Ph.D. degree in electrical engineering from the University of Minnesota, Minneapolis, in 2003. From 2003 to 2005, she was an Assistant Professor of Electrical and Computer Engineering at Auburn University. Since 2006, she has been with the School of Electrical and Computer Engineering at Georgia Institute of Technology, Atlanta, where she is currently an Associate Professor. Her research interests include transceiver designs and diversity techniques for wireless fading channels, cooperative communications, synchronization, and channel modeling, estimation, and equalization.
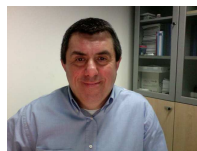
Vincenzo Lottici received the Dr. Ing. degree (cum Laude) and the BTA in electrical engineering both from the University of Pisa in 1985 and 1986, respectively. From 1987 to 1993 he was engaged in the research of sonar digital signal processing algorithms. Since 1993 he has been with the Department of Information Engineering of the University of Pisa, where he is currently an Assistant Professor in Communication Systems. He participated in several international and national research projects, and specifically, from 2005 he has been taking an active role in the standardization activity promoted by ETSI (European Telecommunications Standards Institute) of the physical layer of the mobile radio system TETRA release2. He is or has been TPC member for numerous IEEE conferences in wireless communications and signal processing, such as Globecom2013, WCNC2013, ICUWB2013, WCNC2012, ICUWB2011, ICC2011, WCNC2011, ICASSP2010, PIMRC2010, WCNC2010, CIP2010, Globecom2009, SPAWC2009, EUSIPCO2006, Globecom2006. He joined the Editorial Board of EURASIP Advances on Signal Processing. Dr. Lottici received the Best Paper Award in 2006 for the work "A Theoretical Framework for Soft Information Based Synchronization in Iterative (Turbo) Receivers", EURASIP Journal on Wireless Communications and Networking, April 2005, by the EU-funded project Network of Excellence in Wireless Communications (NEWCOM). His research interests include the broad area of signal processing for communications, with emphasis on synchronization, dynamic resource allocation, cognitive radio and compressive sensing.